ELSEVIER

Journal of Crystal Growth 208 (2000) 401–408

JOURNAL OF CRYSTAL GROWTH

www.elsevier.nl/locate/jcrysgro

Growth of fcc Co in sputter-deposited Co/Au multilayers with (1 1 1) texture

Th. Kehagias[a], Ph. Komninou[a,*], C. Christides[b], G. Nouet[c], S. Stavroyiannis[d], Th. Karakostas[a]

[a]*Department of Physics, Aristotle University, 540 06 Thessaloniki, Greece*
[b]*Department of Engineering Sciences, School of Engineering, University of Patras, 261 10 Patras, Greece*
[c]*LERMAT, UPRESA CNRS 6004, ISMRA, 6 Bd du Marechal Juin, 14050 Caen Cedex, France*
[d]*Institute of Materials Science, NCSR "Democritos", 153 10 Aghia Paraskevi, Greece*

Received 23 July 1999; accepted 1 September 1999
Communicated by R. Kern

Abstract

The growth of Co/Au multilayers on Si(0 0 1)/SiN_x is investigated by means of transmission and high resolution electron microscopy (TEM-HREM) as a function of Co layer thickness. Although there is an amorphous SiN_x buffer layer between the substrate and the multilayer, the growth of alternative Co and Au layers exhibit strong texture with the (1 1 1) planes of Au oriented normal to the growth direction. The multilayer consists of columns that are composed of small misoriented crystals and multiple twins having as twin planes the (1 1 1) planes of growth. Electron diffraction analysis shows that when the Co layers are thinner than the Au layers an average face centred cubic (fcc) lattice is formed throughout the columnar structure of the multilayer, adopting an interplanar *d*-spacing of 0.229 nm along the growth direction. When the Co layer thicknesses become equal or greater than Au thickness then two separate cubic lattices appear due to internal stress relaxation.

PACS: 61.16.Bg; 68.65. + g; 81.15.Cd

Keywords: TEM; Co/Au multilayers; fcc Co; Magnetron sputtering; Low-field GMR

1. Introduction

In recent years, ultrathin magnetic layers or multilayered (MLs) structures comprised of alternating Co and noble metals have attracted a great interest because they exhibit perpendicular magnetic anisotropy [1,2] and quantum size effects leading [3,4] to giant magnetoresistance (GMR). Generally, the dependence of the film morphology on atomic-size mismatch effects at interfaces is of major importance for fundamental and technological reasons [1–4]. In particular, the influence of a large deposit atom on small underlayer atoms, and vice versa, for two elements which are completely immiscible in the bulk has been largely investigated [1,2,5–11]. Especially, ultrathin Co/Au(1 1 1) layers and superlattices have shown

* Corresponding author. Tel.: + 30-31-998195, fax: + 30-31-998061.
E-mail address: komnhnoy@ccf.auth.gr (Ph. Komninou)

0022-0248/00/$ - see front matter
PII: S0022-0248(99)00480-7

a large diversity in magnetic domain sizes [1,2] and related film morphology [5–10] that depend strongly on the deposition conditions used. It was observed [5–9] that surface reconstruction of Au(1 1 1) influences the nucleation and subsequent growth of Co layers. Thus, during growth on Au(1 1 1) surface, depending on the stacking period of the close-packed planes, the Co structure can be either a hexagonal close-packed (hcp), a fcc or a twinned fcc one. Previous TEM and HREM studies of similar Co/Au MLs, grown by other techniques as for instance ultra high vacuum (UHV) physical vapour deposition or molecular beam epitaxy (MBE), have shown a hcp stacking of the close-packed Co planes [5,10,12–16].

Traditionally, sputtering is a simple and rapid method for growth of polycrystalline thin films having a morphology that can be easily adjusted by the deposition conditions. Lately, we have shown [17] that sputter-grown Co/Au MLs, with (1 1 1) texture, exhibit low-field GMR due to low magnetocrystalline anisotropy in Co layers. Analyses of their X-ray diffraction and ^{59}Co nuclear magnetic resonance spectra [18] provided indirect evidence that Co layers are severely expanded along the growth direction and exhibit an unusual Co stacking. A detailed study of the magneto-transport and optical properties [19] as a function of Co layer thickness has also revealed a significant change in the distribution of grain-sizes with profound influences on the variation of the GMR effect. In this study, our aim is to investigate the film morphology and Co crystal structure of the low-field GMR Co/Au MLs as a function of Co layer thickness, using TEM and HREM.

2. Experimental procedure

Magnetron sputtered $[\mathrm{Co}(x\ \mathrm{nm})/\mathrm{Au}(2.5\ \mathrm{nm})]_{30}$ MLs were grown in the Institute of Materials Science of NCSR "Demokritos" on top of Si(0 0 1) substrates with a 100 nm thick SiN_x buffer layer. A high vacuum Edwards E360A sputtering system with a cluster of ATOM-TECH 320-SE planar magnetron sputter sources was used. All samples were deposited in a cryogenically pumped chamber with a base pressure of 8×10^{-5} Pa under an Ar pressure of 0.4 Pa. An RF magnetron gun operating at 30 W with a deposition rate of 0.09 nm/s was used for Co, and DC sputtering at 5 W for Au, resulting in a rate of 0.12 nm/s. All depositions were performed at room temperature.

Specimens for plan view and cross-section electron microscopy (XTEM) were prepared using the standard techniques of mechanical thinning followed by appropriate ion milling. TEM observations were carried out in a Jeol JEM 120 CX electron microscope operated at 120 kV. In the electron diffraction analysis, the 2 2 0 reflection of Si was used as a reference for the precise determination of Au and Co interplanar spacings. Thus, measurements bare a precision of ±0.0015 nm. HREM observations were carried out in a Topcon 002 B electron microscope operated at 200 kV, with a point to point resolution of 0.18 nm and $C_S = 0.4$ mm.

3. Results and discussion

3.1. $[Co(1\ nm)/Au(2.5\ nm)]_{30}$

First, we examine the $[\mathrm{Co}(1\ \mathrm{nm})/\mathrm{Au}(2.5\ \mathrm{nm})]_{30}$ MLs that exhibit the maximum GMR ratio [17]. As in low-field GMR Co/Cu MLs [20], the growth of $[\mathrm{Co}(1\ \mathrm{nm})/\mathrm{Au}(2.5\ \mathrm{nm})]_{30}$ MLs on (0 0 1)Si, with an intervening 100 nm thick SiN_x buffer layer, is strongly textured with the (1 1 1) planes of Au oriented normal to the direction of growth. The MLs exhibit a characteristic columnar mode of growth (Fig. 1a), with a highly twinned structure, where the twin planes are the (1 1 1) planes of growth [17]. The corresponding electron diffraction pattern of the MLs, in Fig. 1b, shows reflections of the [0 1 1] and the [1 1 2] zone axes of Au and the [0 1 1] axis of the Si substrate, with the $1\,1\,\bar{1}$ reflection of Au oriented exactly parallel to the 0 0 4 reflection of Si for both zone axes of Au. These zone axes were observed in all diffraction patterns, which can easily be explained by considering the statistical distribution of the various orientations. Thus, within the large field of view of the selected area aperture of the microscope, one always expects to find columns having these zone axes orientations. The arc-shaped intensity of the

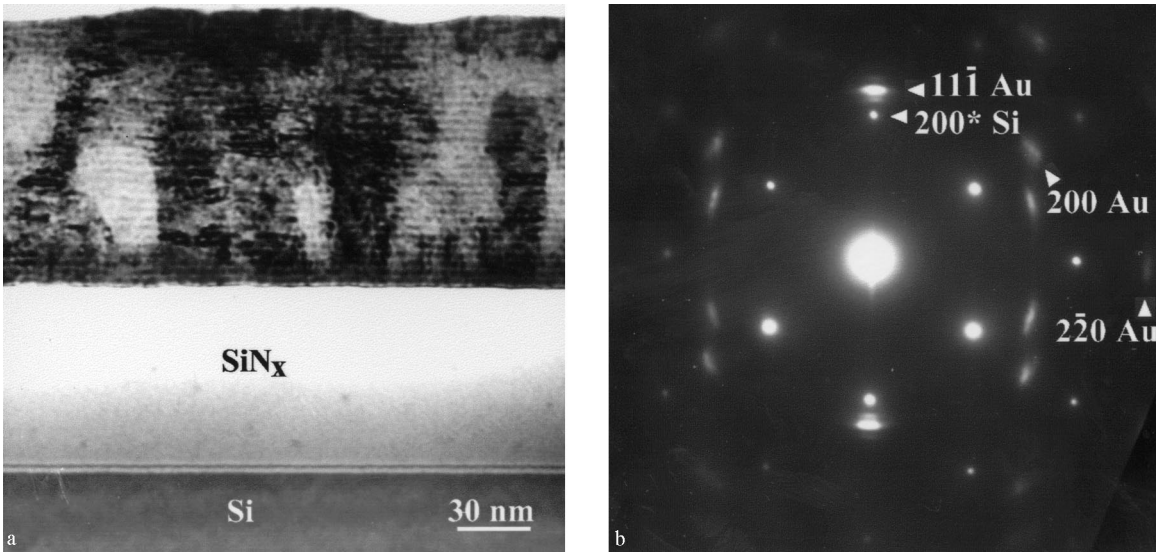

Fig. 1. (a) Bright-field (BF) image illustrating the columnar mode of growth of the [Co(1 nm)/Au(2.5 nm)]$_{30}$ MLs on Si(0 0 1)/SiN$_x$. The Co/Au layers appear as successive bright and dark bands, respectively. (b) Corresponding diffraction pattern where the twinning reflections reveal the existence of multiple twins, having as twin planes the (1 1 1) planes of growth. The 2 0 0* forbidden reflection of Si appears due to double diffraction.

reflections arising from the MLs, as shown in Fig. 1b, indicates that they consist of small misoriented grains within a range of 10°, whereas the satellite reflections around the fundamental 1 1 $\bar{1}$ reflection of Au verify the overall modulated structure. The crystal structure of the MLs is rather homogeneous, since the columns grow unperturbed over many successive Co/Au layers or even from the bottom to the top surface of the MLs. From the diffraction patterns, the d-spacing of the (1 1 1) planes of Au was found to be $d_{1\,1\,\bar{1}}$(Au) = 0.229 nm, which is smaller with respect to the bulk Au value of 0.2355 nm. Also the d-spacing of the 2 0 0 reflection of Au was found to be $d_{2\,0\,0}$(Au) = 0.198 nm, which is reduced by 2.5% relative to bulk Au value of 0.2039 nm. In addition, the interplanar spacing of the 2 $\bar{2}$ 0 reflection of the [1 1 2] zone axis is $d_{2\,\bar{2}\,0}$ (Au) = 0.141 nm, contracted by 2.2% relative to its bulk value of 0.1442 nm. Since the $d_{1\,1\,\bar{1}}$ spacing of Au is reduced by 2.8%, it is concluded that there is an almost isotropic *volume* contraction in the unit cell of Au, that is slightly higher along the normal to the close-packed planes of growth.

The dark-field (DF) image of Fig. 2, taken from a plan view specimen, reveals that the typical columnar diameters are of the order of a few tens of nanometers. Fig. 3 shows the corresponding diffraction pattern, depicting the characteristic 2 $\bar{2}$ 0 ring of polycrystalline Au, as it was expected from the preferred orientation of growth. Another faint ring, closer to the central spot, with a measured d-spacing of 0.249 nm can be indexed as the (1/3) $\bar{4}$ 2 2 reflections of Au (theoretical value of d = 0.2496 nm). These reflections, although forbidden, often appear in gold crystals and their presence is due to twins and microtwins between the columnar grains, that are misoriented relative to the ⟨1 1 1⟩ direction of growth [14,16] by 10–15°. In Fig. 3, the appearance of the faint 3 1 1 ring of Au can be attributed to the same reasons. It is interesting to note, that the $d_{2\,2\,0}$(Au) = 0.144 nm measured from the plan view diffraction pattern is very close to the bulk value. This is due to strain relaxation inside the MLs, since the plan view specimens were perforated by ion-milling and the substrate was completely removed in the transparent to the electron

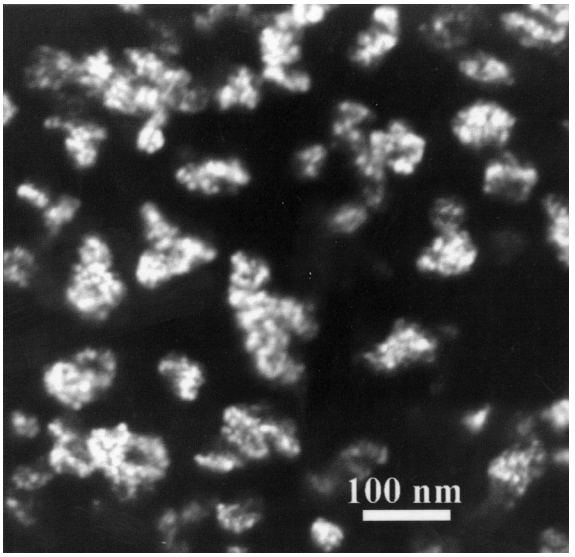

Fig. 2. Dark-field (DF) image of a plan view specimen of $[Co(1\ nm)/Au(2.5\ nm)]_{30}$ MLs, showing that the diameters of the crystal columns are of the order of a few tens of nanometers.

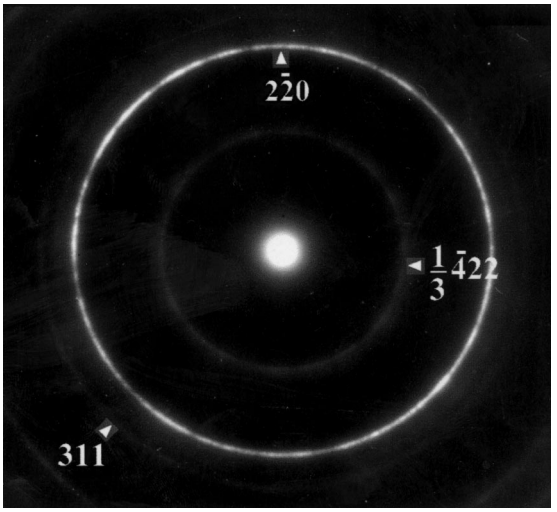

Fig. 3. Diffraction pattern from a plan view specimen of $[Co(1\ nm)/Au(2.5\ nm)]_{30}$ MLs depicting characteristic rings of polycrystalline Au, whereas no rings corresponding either to hcp or to fcc Co are identified.

beam area of the specimen. However, no characteristic polycrystalline rings of hcp or fcc Co are identified in the diffraction patterns of the plan view specimens.

All of the above, in conjunction with the absence of separate reflections from hcp or fcc Co in the diffraction patterns of the XTEM specimens, show that an average fcc lattice is formed throughout the columnar structure of the MLs and thus Co exhibits a cubic structure. Therefore, we concluded that Co layers were grown epitaxially over Au and that the d-spacing of the (1 1 1) planes of Co, along the direction of growth, should be severely expanded in order to conform with the d-spacing of the (1 1 1) planes of the average lattice, which is $\langle d_{1\,1\,1}\rangle = 0.229$ nm. In a first approximation, assuming that there are distinct nanocrystalline Co layers, the $d_{1\,1\,1}$ of Co can be calculated from the expression $\langle d_{1\,1\,1}\rangle = \Lambda/(N_{Au} + N_{Co})$, where Λ is the bilayer thickness and N_{Au} and N_{Co} are the numbers of atomic planes of Au and Co per bilayer, respectively. Using $\Lambda = 3.5$ nm and $N_{Au} = (2.5/0.2355\ nm) = 10.62$ atomic planes of Au in one bilayer, the expression gives a N_{Co} of 4.67 Co atomic planes and thus $d_{1\,1\,1}(Co) = (1\ nm/4.67) = 0.214$ nm, that is larger than the 0.205 nm of bulk fcc Co. The expansion of $d_{1\,1\,1}(Co)$ spacing along the growth direction is 4.4% and induces severe strain in the Co layers, reducing the atomic density of Co. Since the data provide evidence for an epitaxial growth of Co on Au, then a *volume* expansion of the Co unit cell is expected, being more prominent along the growth direction.

3.2. *[Co(3 nm)/Au(2.5 nm)]$_{30}$*

The bright-field (BF) image of Fig. 4 shows that for $[Co(3\ nm)/Au(2.5\ nm)]_{30}$ MLs, with Co layer thickness larger than Au layer thickness, the samples exhibit a similar texture as in the previous case. A columnar and twinned, overall, structure is also observed here, with the same (1 1 1) twin planes. However, plan view micrographs (Fig. 5) show a bimodal distribution of grain sizes with a larger fraction of small grains relative to the previous case. In cross-section specimens, the electron diffraction pattern of the MLs (Fig. 6) contains reflections from the [0 1 1] and the [1 1 2] zone axes of Au and well-resolved reflections from Co, oriented exactly parallel to all the Au reflections. It was found that the value of $d_{1\,1\,\bar{1}}(Au) = 0.233$ nm is much closer to the bulk value in contrast to the

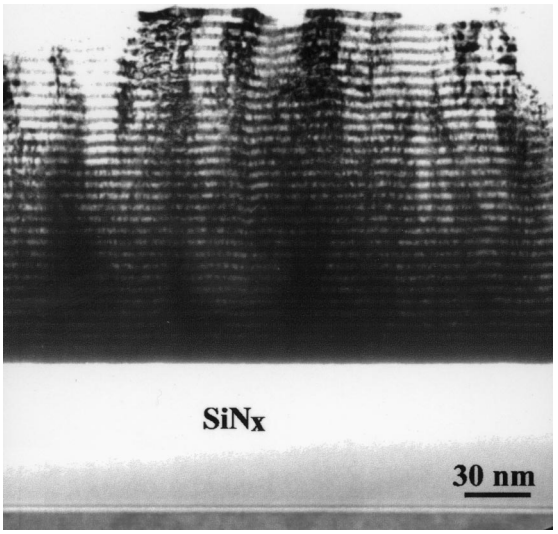

Fig. 4. BF image illustrating the columnar growth of the $[Co(3\ nm)/Au(2.5\ nm)]_{30}$ MLs on $Si(0\ 0\ 1)/SiN_x$. Here, the crystal columns appear thinner, indicating that they consist of grains having smaller diameters.

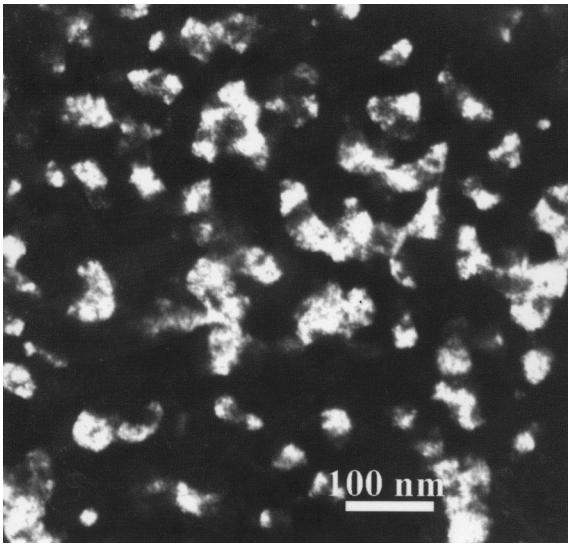

Fig. 5. DF image of a plan view specimen of $[Co(3\ nm)/Au(2.5\ nm)]_{30}$ MLs, showing a larger fraction of small diameter columns than the previous case.

results of the previous case. The d-spacing of the $\bar{2}\,2\,0$ reflection was found to be $d_{\bar{2}\,2\,0}(Au) = 0.143$ nm which is contracted by 1% from its bulk

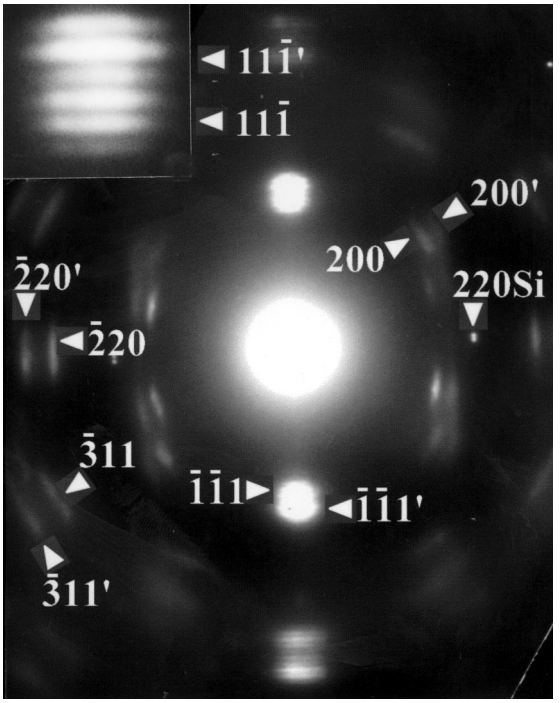

Fig. 6. Diffraction pattern from a XTEM specimen of $[Co(3\ nm)/Au(2.5\ nm)]_{30}$ MLs. Separate Co reflections (primed indices) are visible, aligned in parallel to the Au reflections, that belong to the [0 1 1] and [1 1 2] zone axes. Twinning reflections of both elements are also aligned in parallel.

value. Thus, an isotropic volume contraction of Au unit cell is still present.

To determine whether Co adopts a fcc or a hcp structure the ratios of the relative distances from the central spot and the angles between the Co reflections were estimated. In this way it is possible to distinguish whether the expanded $d(Co) = 0.211$ nm value of the first-order reflection, relates to the $d_{1\,1\,1}$ of fcc Co (0.205 nm) or the $d_{0\,0\,0\,2}$ (0.2035 nm) of hcp Co. Since the Co and Au reflections are oriented in parallel, then the reflections of Co in Fig. 6 can be assigned to the [0 1 1] and the [1 1 2] zone axes of *cubic* Co. In the first zone axis, the measurements give a relative ratio of 1.15 and an angle of 55° between the $2\,0\,0/1\,1\,\bar{1}$ reflections, which are very close to the theoretical 1.155 and 54.74° values. In the [1 1 2] zone axis, the relative ratios between the $\bar{2}\,2\,0/\bar{1}\,\bar{1}\,1$ and the $\bar{3}\,1\,1/\bar{1}\,\bar{1}\,1$ reflections are determined to be 1.64 and 1.93,

respectively, in agreement with the theoretical values of 1.633 and 1.915. The measured angles are 90° and 59°, respectively, which are also in excellent agreement with the theoretical values of 90° and 58.52°. If the Co structure is *hexagonal* the reflections of Co in Fig. 6 should belong to the [0 1 $\bar{1}$ 0] and the [2 $\bar{1}$ $\bar{1}$ 0] zone axes, taking into consideration an epitaxial growth. For the first zone axis, the theoretical distance ratio between the 2 $\bar{1}$ $\bar{1}$ 0/0 0 0 2 reflections is 1.587. This ratio is far from the 1.64 measured value, although the angle between these reflections is 90° which matches the theoretical one. However, the measured distance ratio between the 2 $\bar{1}$ $\bar{1}$ $\bar{2}$/0 0 0 $\bar{2}$ reflections is 1.93, instead of the theoretical 1.876 value, and the corresponding angle is 59°, instead of the theoretical 57.79° value. For the [2 $\bar{1}$ $\bar{1}$ 0] zone axis, a relative ratio of 1.15 and an angle of 55° are measured between the 0 1 $\bar{1}$ 1/0 0 0 2 reflections, whereas the theoretical values are 1.045 and 61.38°, respectively. The 0 1 $\bar{1}$ 0-type reflections that belong to this zone axis could not be identified in the diffraction patterns.

A diffraction pattern from a plan view specimen (Fig. 7) shows the 2 $\bar{2}$ 0 ring of polycrystalline Au with a $d_{2\,\bar{2}\,0}$(Au) = 0.143 nm, in agreement with that measured from cross-section specimens. This experimental value is still smaller than the theoretical value of 0.1442 nm. Thus, despite the perforation of the specimen, a partially relaxed state of Au layers is expected due to larger thickness of the MLs. Next to 2 $\bar{2}$ 0 ring of Au a fainter ring with $d = 0.129$ nm appears, that can be identified as the 2 $\bar{2}$ 0 ring of *cubic* Co (theoretical value $d_{2\,\bar{2}\,0}$(Co) = 0.1256 nm) by taking into account a moderate expansion of Co lattice parameters. If the Co structure is *hexagonal* this ring should correspond to the 1 1 $\bar{2}$ 0 reflection of polycrystalline Co, having a theoretical $d_{1\,1\,\bar{2}\,0}$(Co) = 0.1253 nm, close to the measured value as well. In that case the viewing direction should lie parallel to the [0 0 0 1] zone axis of Co, that includes the strong 1 0 $\bar{1}$ 0-type reflections with a $d_{1\,0\,\bar{1}\,0}$(Co) = 0.217 nm. However, no such ring is detected in plan view diffraction patterns. The appearance of the faint (1/3) $\bar{4}$ 2 2, 1 1 1 and 3 1 1 rings of Au can be explained again as in the previous case.

It is obvious from the electron diffraction analysis, that the experimental data are in agreement with the theoretical values only if we consider Co to exhibit a cubic symmetry. Since the reflections of cubic Co are oriented exactly parallel to the corresponding reflections of Au, it is verified that Co layers grow epitaxially on Au. However, an average lattice cannot be considered when the Co layer thickness is close or larger than the Au layer thickness, because the diffraction patterns show distinct Co reflections with $d_{1\,1\,1}$(Co) and $d_{1\,1\,1}$(Au) spacings close to their bulk values. The inset in Fig. 6 shows an enlarged area of the diffraction pattern, where the satellite reflections arising from the bilayer modulation can be resolved next to the first-order 1 1 $\bar{1}$ reflections of Au and Co. As mentioned above, the *d*-spacing of (1 1 1)Co planes along the growth direction was found to be 0.211 nm, that is expanded by 2.9% relative to the corresponding bulk value. Also, the $d_{2\,2\,0}$ of Co is 0.129 nm, expanded by 2.7% relative to its bulk value. Thus, a *volume* expansion of the Co unit cell is detected, that is slightly higher along the normal to the close-packed planes of growth, but overall can be considered as isotropic expansion. The Co lattice expansion is reduced as the Co layer thickness increases and the strain is gradually relaxed.

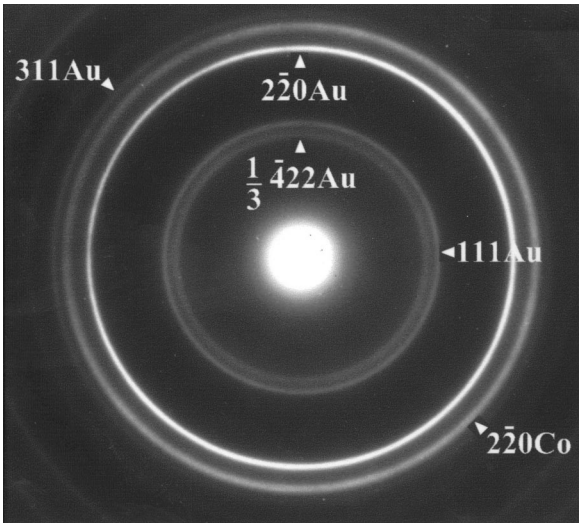

Fig. 7. Diffraction pattern from a plan view specimen of $[Co(1\,nm)/Au(2.5\,nm)]_{30}$ MLs depicting separate polycrystalline rings of Co next to the corresponding rings of Au.

3.3. The growth process

In order to understand the growth process of the MLs deposition, HREM observations were performed in both types of specimens. These observations were performed at the same orientation as the conventional TEM observations. Two typical cases are presented in Figs. 8 and 9. As it is seen from both HREM images, the growth of Co progresses with a stacking sequence of close-packed planes which are oriented parallel to the surface of the substrate successively with the (1 1 1) planes of Au. The MLs structures contain planar defects, as stacking faults and twin boundaries, that are mostly lying parallel to the planes of growth. The existence of these planar defects within the Co layers, can modify the stacking sequence of the close-packed planes and are expected to alter the stacking along the direction of growth from fcc to hcp and vice versa. However, this phenomenon will be localised in the defected area only and, generally, is not expected to influence the observed long-range fcc symmetry inside the Co layers.

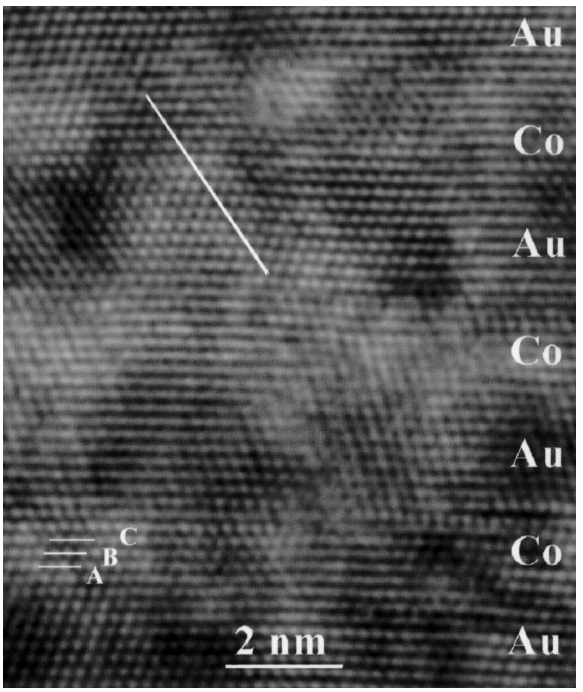

Fig. 8. HREM image of the $[Co(1\,nm)/Au(2.5\,nm)]_{30}$ MLs illustrating the ABCABC stacking sequence of the close-packed planes in Co layers. The white inclined solid line depicts the trace of a $(\bar{1}\,1\,1)$ plane that transverses successive Au and Co layers without any change in orientation.

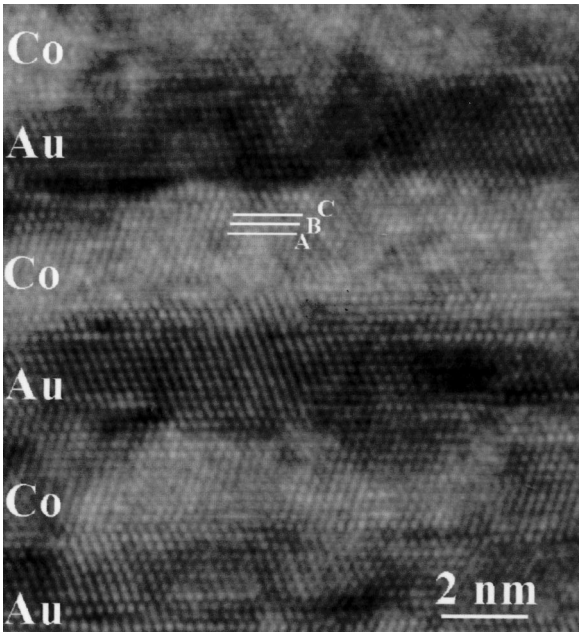

Fig. 9. HREM image of the $[Co(3\,nm)/Au(2.5\,nm)]_{30}$ MLs, where the ABCABC stacking sequence of the close-packed planes in Co layers indicates the formation of fcc Co during growth. The $d_{1\,1\,1}$(Co) is expanded due to the influence of the Au lattice.

As it is illustrated in Fig. 8, the observed stacking sequence in the undefected areas of both Co and Au layers of the $[Co(1\,nm)/Au(2.5\,nm)]_{30}$ MLs is ABCABC and the *d*-spacings of the (1 1 1) planes of Co and Au are more or less the same, indicating a large expansion of the $d_{1\,1\,1}$(Co) relative to its bulk value. The white inclined solid line depicts the trace of a $(\bar{1}\,1\,1)$ plane that transverses successive Au and Co layers without any change in orientation. This observation supports the results of the electron diffraction analysis, concerning the existence of an average fcc lattice in this type of MLs. As it is shown in Fig. 9, the stacking sequence of close-packed planes in Co layers of the $[Co(3\,nm)/Au(2.5\,nm)]_{30}$ MLs is also ABCABC, indicating the formation of fcc Co during growth. However, the $d_{1\,1\,1}$(Co) is here less expanded

relative to its bulk value, whereas $d_{1\,1\,1}$(Au) is rather close to its corresponding bulk value. This observation also supports the electron diffraction results and excludes the existence of an average lattice in this type of MLs.

4. Conclusions

Magnetron sputtering has been successfully used to produce high-quality thin Co/Au MLs. The MLs present a well-defined layered morphology, exhibiting textured columnar growth with a twinned crystal structure. For Co layer thicknesses of 1–3 nm and constant Au layer thickness of 2.5 nm, the Co layering corresponds to fcc stacking epitaxially grown on the (1 1 1) planes of Au. However, depending on the Co layer thickness, an important difference in the structure was verified. In thinner (1 nm) Co layers an expanded fcc lattice is obtained, while the Au lattice is compressed. In this case, both materials tend to form an average fcc lattice with an interplanar spacing along the growth direction closer to Au *d*-spacing. For thicker (3 nm) Co layers an expanded fcc lattice occurs as well, but in this case the expansion is significantly reduced and the Au lattice is only slightly contracted. No average lattice is formed in this case and along the growth direction both elements exhibit interplanar spacings closer to their bulk values.

References

[1] M. Speckmann, H.P. Oepen, H. Ibach, Phys. Rev. Lett. 75 (1995) 2035.
[2] M. Dreyer, M. Kleiber, A. Wadas, R. Wiesendanger, Phys. Rev. B 59 (1999) 4273.
[3] S.S.P. Parkin, R. Bhadra, K.P. Roche, Phys. Rev. Lett. 66 (1991) 2152.
[4] V. Grolier, D. Renard, B. Bartelian, P. Beauvillain, C. Chappert, C. Dupas, J. Ferre, M. Galtier, E. Kolb, M. Mulloy, J.P. Renard, P. Veilet, Phys. Rev. Lett. 71 (1993) 3023.
[5] T. Kingetsu, K. Sarai, Phys. Rev. B 48 (1993) 4140.
[6] T. Kingetsu, K. Sarai, J. Appl. Phys. 73 (1993) 7622.
[7] T. Kingetsu, K. Sarai, J. Appl. Phys. 74 (1993) 6308.
[8] T. Kingetsu, Jpn. J. Appl. Phys. 36 (1997) L1658.
[9] B. Voigtlander, G. Meyer, N.M. Amer, Phys. Rev. B 44 (1991) 10354.
[10] N. Marsot, R. Belkhou, H. Magnan, P. Le Fevre, C. Guillot, D. Chandersis, Phys. Rev. B 59 (1999) 3135.
[11] I. Meunier, G. Treglia, J.-M. Gay, B. Aufray, B. Legrand, Phys. Rev. B 59 (1999) 10910.
[12] D. Renard, G. Nihoul, Philos. Mag. B 55 (1987) 75.
[13] R. Clark, S. Elagoz, W. Vavra, E. Schuler, C. Uher, J. Appl. Phys. 70 (1991) 5775.
[14] N. Mliki, K. Abdelmoula, G. Nihoul, C. Marliere, D. Renard, Thin Solid Films 224 (1993) 14.
[15] F. Hakkens, A. De Veirman, W. Coene, F.J.A. den Broeder, J. Mater. Res. 8 (1993) 1019.
[16] H. Ardhuin, E. Snoeck, M.-J. Casanove, J. Cryst. Growth 182 (1997) 394.
[17] S. Stavroyiannis, C. Christides, Th. Kehagias, Ph. Komninou, Th. Karakostas, D. Niarchos, J. Appl. Phys. 84 (1998) 6221.
[18] C. Christides, S. Stavroyiannis, D. Niarchos, M. Wojcik, S. Nadolski, E. Jedryka, Phys. Rev. B 59 (1999) 8812.
[19] C. Christides, S. Stavroyiannis, D. Niarchos, M. Gioti, S. Logothetidis, Phys. Rev. B, submitted for publication.
[20] C. Christides, S. Stavroyiannis, N. Boukos, A. Travlos, D. Niarchos, J. Appl. Phys. 83 (1998) 3724.